Reliability Enhancement of Wafer Level Packages with Nano-Column-Like Hollow Solder Ball Structures

Ronak Varia and Xuejun Fan
Department of Mechanical Engineering
Lamar University
PO Box 10028, Beaumont, TX 77710, USA
Tel: 409-880-7792; E-mail: xuejun.fan@lamar.edu

Abstract

In this paper, hollowed solder ball structures in wafer level packages are investigated. Detailed 3-D finite element modelling is conducted for stress and accumulated inelastic strain energy density or creep strain analysis. Three cases are studied in this paper: a regular solder ball, a solder ball with a polymer core of sphere shape, and a hollowed solder ball. Two different creep models are applied: 1) anand model; and 2) hyperbolic sine creep model. Testing data of polymer-cored solder ball WLP are used for verification. Hollowed ball WLP appears to have further improved thermal-cycling performance. When anand model is used, some unexpected results are obtained: 1) maximum inelastic strain energy density and von Mises stress occur in the balls of the middle of the diagonal row; and 2) von Mises stress is almost equally distributed among all balls. However, when hyperbolic sine creep model is used, the obtained results are consistent with the observations in conventional solder ball WLP. Nevertheless, both creep models predict the significant reduction in solder ball stress and accumulated creep strain or inelastic strain energy density for hollow ball WLP. Existing experimental results of polymer-cored WLP from literature can indirectly validate the benefit from hollowed balls.

Introduction

Wafer level packages (WLPs) are primarily used for low pin-count and small die-size applications, such as analogue and power management devices, image sensors, integrated passives, and memory chips in mobile electronic devices. WLP is one of the fast growing segments in semiconductor packaging industry due to the increasingly demands of function integration, miniaturization and cost reduction.

It is well understood that solder ball thermo-mechanical reliability is of critical concern of WLPs with larger die packages [1-3]. The ability of solder joints to survive the required thermal cycle testing has limited the WLPs to the products having relatively small die sizes and a small number of I/O [4]. The intrinsic difference in the coefficient of thermal expansion (CTE) between silicon (~2.6ppm/°C) and PCB (~17ppm/°C) determines that the solder ball thermal cycling fatigue performance is limited by die-size.

A variety of WLP technologies have been developed in recent years to improve the thermo-mechanical reliability performance for large array WLPs. Standard WLP, which is similar to a typical flip chip technology, has evolved with the incorporation of redistribution layer (RDL) process [5-8], copper post process [9], and compliant layer process [10]. These WLP structures have demonstrated the significant enhancement and improvement on solder joint reliability. But new failure modes, such as RDL cracking and delamination, may appear.

There are many factors that affect the thermo-mechanical reliability of solder joints in WLP packages. Polymer film layer, in which redistribution traces are embedded, serve as a stress buffer layer to reduce the stress level in solder joints. It is generally conceived that the high compliance of polymer film (e.g., low Young's modulus) results in solder joint stress reduction [10]. Ball shape, geometry, standoff height, and material also play an important role in thermo-mechanical performance of WLPs [11-16]. Previous works have demonstrated that a greater standoff height with a slim ball-shape offer improved reliability performance. In addition, PCB design and material selection also contribute significantly to WLP's reliability. Recently, polymer-cored solder balls have been applied to WLPs [11,12]. A plastic core solder ball consists of a large polymer core coated by a copper layer and covered with eutectic and/or lead-free solder. The main advantages of such a structure are higher reliability due to the relaxing of stress by the polymer core and a defined ball height after reflow. These structures could improve the solder ball reliability significantly.

In this paper, hollowed solder ball structures in wafer level packages are investigated. Three cases are studied in this paper: a regular solder ball, a solder ball with a polymer core of sphere shape, and a hollowed solder ball. A detailed 3-D finite element model is constructed for the analysis. To investigate the effect of constitutive models for solder alloys, different creep models are applied. The results are compared among three cases, and the testing data for polymer-cored solder ball WLP are used for verification.

Hollow Solder Balls

To improve the compliance of WLP structures, solder balls may be constructed with nano-size column like or honeycomb like structures. Some possible configurations of 'hollow solder balls' are illustrated in Figure 1. These new ball structures would need new process to realize. The rapid advances in nano-material and nano-manufacturing developments would make it happen in the near future. The 'ball' materials are not limited to 'solder alloys'.

In this paper, to be able to compare directly with the existing solder joint structures, a hollowed solder ball, which has the exact same geometry of a regular solder ball, is investigated. Three cases are studied in this paper: a regular solder ball, a solder ball with a polymer core of sphere shape, and a hollow solder ball, as shown in Figure 2. For polymer-cored ball, a plastic core solder ball consists of a large polymer core (called DVB) coated by a copper layer and covered with eutectic and/or lead-free solder.

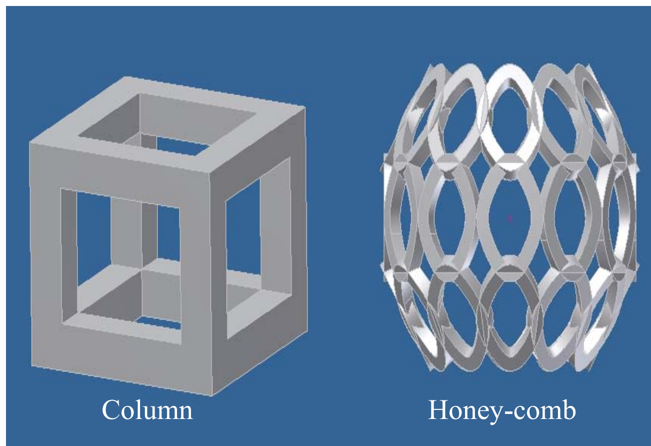

Figure 1 Nano-size column-like or honeycomb-like interconnects to replace solder balls

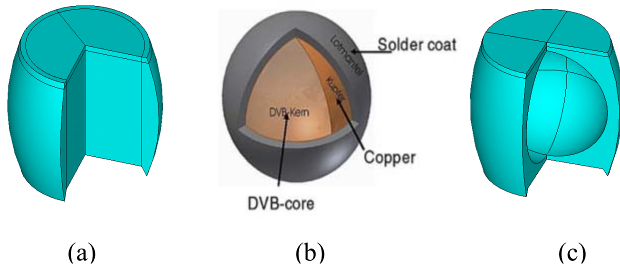

(a) (b) (c)

Figure 2 Three solder ball structures a) a regular solder ball; b) a polymer-cored solder ball; and c) a hollowed solder ball

Solder Alloy Creep Models

To study the behavior of solder balls under thermal cycling, it is important to select appropriate creep models. In this study, two creep models are applied: 1) Anand model; and 2). hyperbolic sine creep model.

Anand Model

To analyze rate dependent creep behavior of solder alloy, Anand model [17] is used:

$$d^p = Ae^{-\frac{Q}{R\theta}}\left[\sinh\left(\zeta\frac{\sigma}{s}\right)\right]^{\frac{-1}{m}} \quad (1)$$

where,

$$s = \{h_0\,(|B|)^a \mathrm{sgn}(B)\}d^p$$

$$B = 1 - \frac{s}{s^*}$$

$$s^* = s\left[\frac{d^p}{A}e^{\frac{Q}{R\theta}}\right]^n \quad (2)$$

where, d = effective inelastic deformation rate,

σ = the effective Cauchy stress,

s = the deformation resistance,

s* = the saturation value of deformation resistance,

ś = the time derivative of deformation resistance,

θ = the absolute temperature.

Equation (1) gives the nine material constants for rate-dependent visco-plastic description, and Table 1 lists those constants used in this study.

Hyperbolic Sine Creep Model

Hyperbolic sine creep model follows the equation [19]

$$\varepsilon_{cr} = C_1[\sinh(C_2\sigma)]^{C_3}e^{-C_4/T} \quad (3)$$

where, Ci (i=1,2,3,4) is the material constants. For SnAgCu alloy, the constants were determined as C1 = 441000, C2 = 0.005, C3 = 4.2 and C4 = 5412 [19].

Table 1 Material parameters of viscoplastic Anand model [18]

Name	Value
s0, MPa	1.3
Q/R, K	9000
A, sec-1	500
ξ	7.1
M	0.3
h0, MPa	5900
s^, MPa	39.4
N	0.03
α	1.5

Finite Element Models

A 12×12 array wafer level package with copper post interconnect is considered. The pitch of solder ball is 0.5mm and, thus the die size is 6mm×6mm. Due to the symmetry, only the one-eighth of the entire model is used in building finite element model, as shown in Figure 3. It is known that the outermost solder balls along the diagonal directions are the most critical ones with the largest thermo-mechanical stresses. Therefore, the PCB size in the model is extended at least 2.5 times of the package size to reduce the possible edge effect of PCB board on the outermost solder ball stresses. The detailed geometry information is given in Table 2. All geometries remain the same for all three cases under study. For hollowed solder ball, the diameter of hollowed portion is 250 µm, which is same as the diameter of polymer core.

In the finite element model, a fixed-thickness layer of 10 µm is created at the top of solder ball for volume averaging to minimize the mesh size effect. The per-cycle inelastic strain (or creep strain) or inelastic strain energy density is used as damage metrics to evaluate solder joint reliability [20-26]. For example, the volume averaged inelastic energy density over the 10 µm thin disk is defined as follows,

$$\Delta W_{ave} = \frac{\sum \Delta W_i V_i}{\sum V_i} \quad (4)$$

where, $\Delta W_{ave} =$ average inelastic strain energy density accumulated per cycle for fixed thickness layer elements, $\Delta W_i =$ strain energy density accumulated per cycle for each element i, and Vi = volume of each element i.

In the present study, 125°C is used as stress-free temperature for thermal cycling loading from -45°C to 125°C [20]. The time duration each cycle is 60 minutes, with 15 minutes during ramp up and down, and 15 minutes of dwell at -40°C and 125°C, respectively.

In this study all other materials are modeled as linear elastic, whose properties are given in Table 3.

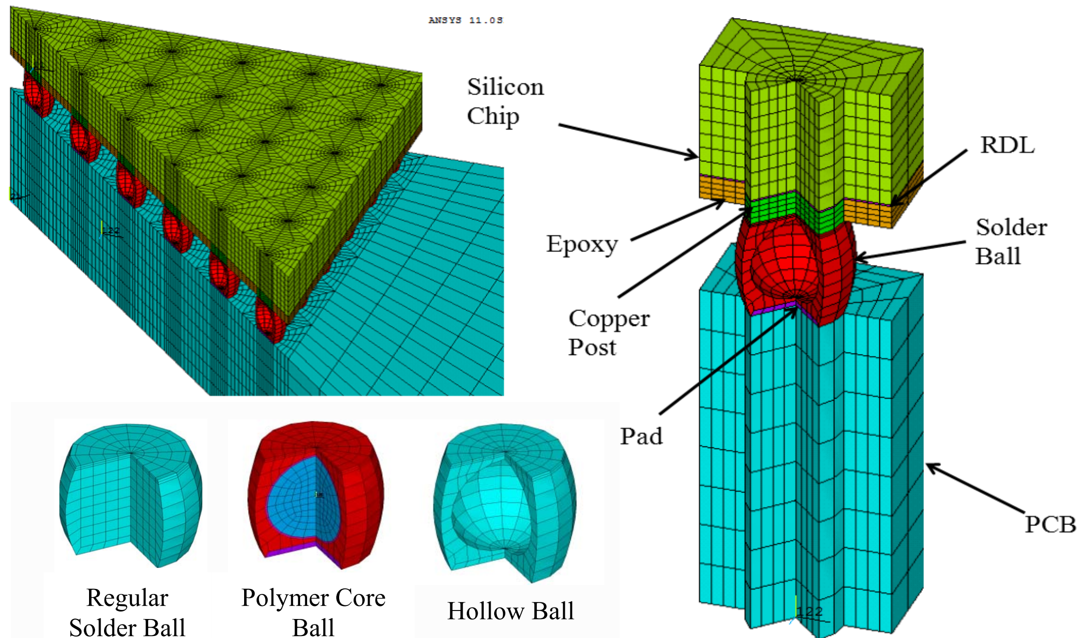

Figure 3 One-eighth finite element model for a 12×12 array wafer level package with different ball structures

Table 2 Geometrical dimensions of the WLP packages

	Dimensions (μm)		
Solder ball type	Regular Solder Ball	Polymer-core Ball	Hollow Ball
Silicon thickness	350	350	350
Solder ball diameter	300	300	300
Solder ball standoff height	295	295	295
Solder ball opening diameter	250	250	250
PCB pad diameter	250	250	250
PCB thickness	1000	1000	1000
Wafer Passivation thickness	4	4	4
Epoxy/Copper post thickness	70	70	70
Polymer core diameter	-	240	-
Diameter of hollow portion	-	-	250

Table 3 Material property details of the materials in a WLP

Materials	Young's modulus (GPa)	CTE (ppm/°C)	Poisson's ratio
Silicon	130	2.6	0.28
Passivation	105	11	0.24
Epoxy	14	20	0.24
Polyimide	1.2	52	0.34
Cu post	130	16.8	0.3
Solder ball	50	24.5	0.35
PCB pad	130	16.8	0.34
PCB	25	16	0.39
Polymer core	4.70E+03	4.00E-05	0.38

Results

Inelastic Strain Energy Density and von Mises Stress

Table 4 shows the results of the inelastic strain energy density and von Mises stress for three solder ball structures with Anand creep model used. The displayed results are for the outermost ball in the diagonal direction. Both the maximum and the averaged results are obtained. The averaged values are calculated according to equation (4). The solder ball height is considered as the height when polymer cored ball is used for the same diameter of solder ball. In reality, the height of the regular solder ball with the same diameter (shown in Table 3) is around 235μm. Nevertheless, Table 4 clearly shows the significant reduction in both inelastic strain

energy density and stress in solder balls when hollow structure is applied. Hollowed ball structures increase the compliance of the WLP during thermal cycling, and thus, less stresses are exerted on the solder ball interface with copper post. On the other hand, it is observed that for polymer-cored solder balls, complicated results are obtained. Maximum stress in polymer-cored solder balls does not show much reduction, especially after the averaged process is done. This indicates that for polymer-cored ball structures, stress distribution is more 'uniform' than regular balls. Such results are also confirmed from inelastic strain energy density. The averaged inelastic strain energy density for polymer-cored balls is almost same with the regular balls when the same height is used. In actual applications, the ball height is much less for the regular balls, which will reduce the thermal cycling performance. We will also consider the effect of creep models in the later part of this section.

Table 4 Comparison of the inelastic strain energy density and von Mises stress for three cases

Ball Type	Anand model		
	Regular	Polymer-cored	Hollowed
Ball Height (μm)	295	295	295
Max von Mises Stress (MPa)	63.20	54.71	36.8
Max Plastic Work (MPa)	2.62	1.54	0.40
Avg. von Mises Stress (MPa)	34.09	30.72	26.49
Avg. Plastic Work (MPa)	0.23	0.20	0.07

Maps of Inelastic Strain Energy Density and von Mises Stress

Figures 4 and 5 show the maps of the averaged and maximum inelastic strain energy density of an one-eighth segment in a 12×12 array WLP with hollowed balls. For the averaged strain energy density, DNP effect appears and the outermost ball in the diagonal direction has the maximum averaged inelastic strain energy density. However, unexpectedly, the maximum inelastic strain density occurs in the ball in the middle of the row along the diagonal direction Figures 6 and 7 plots the maps of the averaged von Mises stress and maximum von Mises stress. The similar patterns are observed. Moreover, it can be found that the stresses are more equally supported by all of balls, despite the differences among those balls. Those results are very different from a WLP package with regular balls. It is noted that the above results are obtained based on Anand model. In the next section the hyperbolic sine law creep model is used.

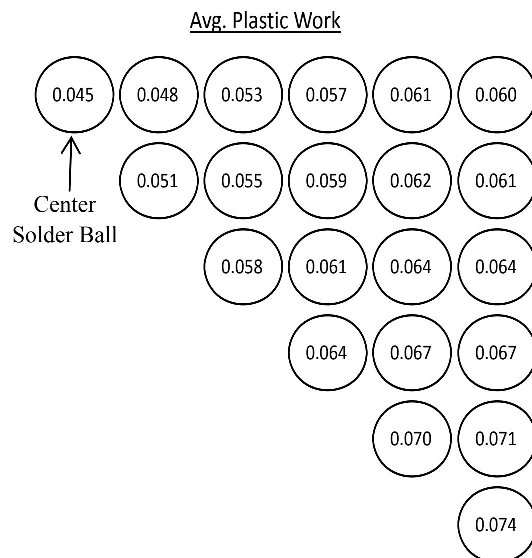

Figure 4 Map of the averaged inelastic strain energy density in hollowed ball WLP

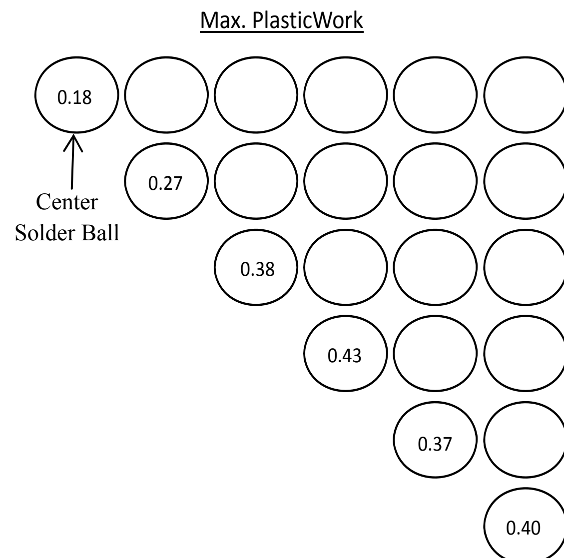

Figure 5 Maximum inelastic strain energy density distribution along diagonal direction in a hollowed ball WLP

Effect of Creep Models

To verify the above results, the hyperbolic sine creep model of equation (3) is applied. Table 5 shows the results of the creep strain intensity and von Mises stress for three solder ball structures with hyperbolic sine creep model used. The displayed results are for the outermost ball in the diagonal direction. Both the maximum and the averaged results are obtained, and the averaged values are calculated according to equation (4). The solder ball height for the regular ball case is considered as the actual height of 234μm. Table 5 clearly shows the benefit using either polymer cored or hollowed balls. However, the results are different from the results obtained using Anand model (Table 4). The results for polymer-cored case are closer to the hollowed case. Furthermore, Figures 8 and 9 plot the distributions of maximum creep strain intensity and von Mises stress along

diagonal balls. The results are consistent with the DNP effects seen in regular balls. It is noted that the magnitude of von Mises stress with hyperbolic sine law is much higher than the anand model, even though both models are for SnAgCu alloy and the same elastic properties (Young's modulus and Possion's ratio) are used.

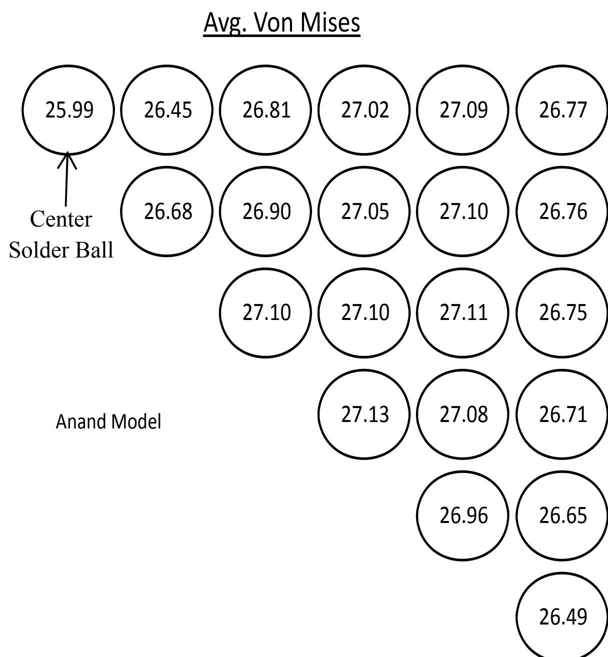

Figure 6 Map of the averaged von Mises stress in hollowed ball WLP

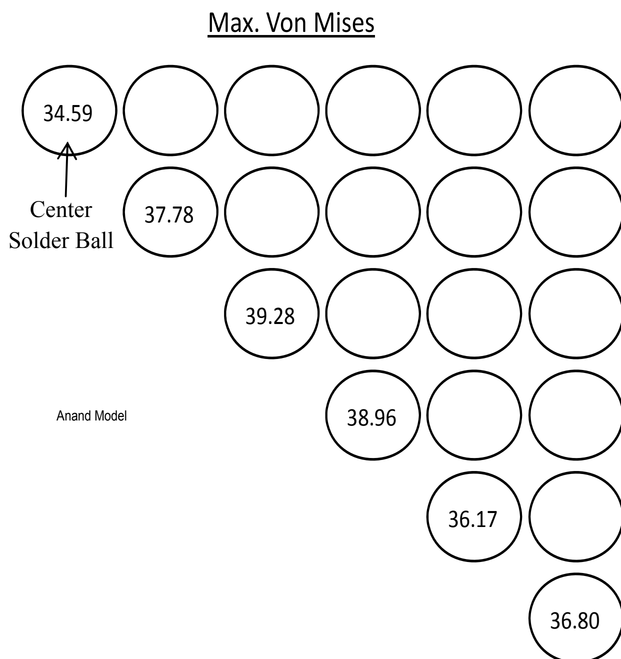

Figure 7 Maximum von Mises stress distribution along diagonal direction in a hollowed ball WLP

Table 5 Comparison of the inelastic strain energy density and von Mises stress for three cases

Ball Type	Hyperbolic sine creep model		
	Regular	Polymer-cored	Hollow
Ball height (μm)	234	295	295
Max von Mises Stress (MPa)	341.62	270.26	256.28
Max creep strain intensity	5.10E-09	1.9E-09	1.5E-09
Avg. von Mises stress (MPa)	140.2	116.88	105.11
Avg. creep strain intensity	3.60E-10	2.2E-10	1.9E-10

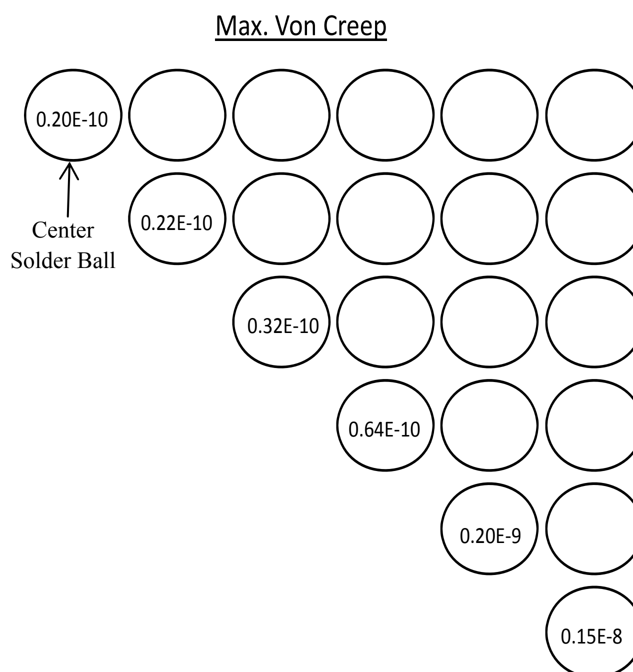

Figure 8 Maximum creep strain intensity distribution along diagonal direction in a hollowed ball WLP

Experimental Verification

The experimental reliability performance of polymer-cored solder balls may be used for an indirect verification for hollowed solder ball performance. Weibull distribution for a WLP with polymer cored solder balls [12] with conventional solder ball WLP is given in Figure 10 for the failure rate in thermal cycling. At N50 polymer-cored solder ball reliability shows the doubled life compared to the conventional solder ball. These experimental results are consistent with simulation predictions, shown in Tables 4 and 5, respectively. Since hollow solder balls can further reduce the stresses, we expect a further improvement in fatigue life with hollowed ball structures.

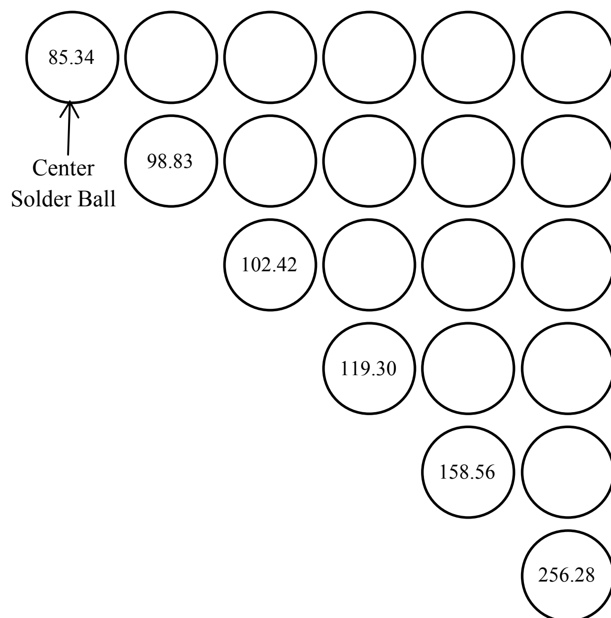

Figure 9 Maximum von Mises stress distribution along diagonal direction in a hollowed ball WLP

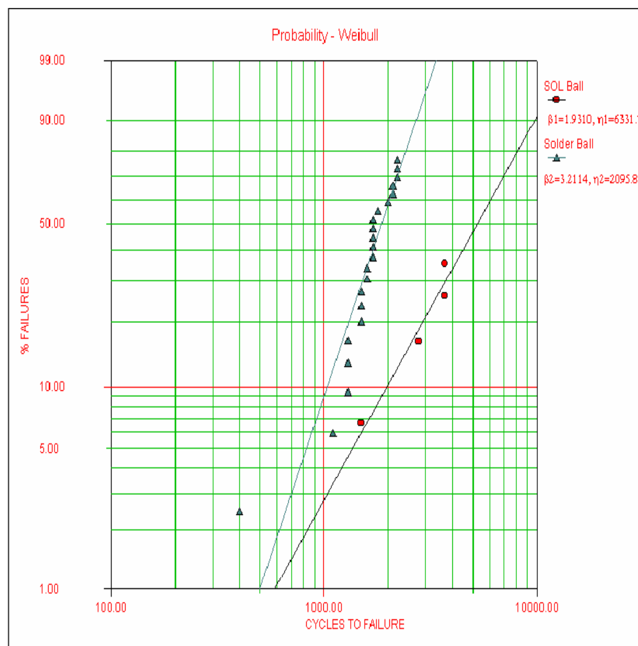

Figure 10 Weibull distribution to failure for polymer-cored WLP [12]

Conclusions

Hollowed ball WLP appears to have further improved thermal-cycling performance due to its compliance. When anand model is used, some unexpected results are obtained: 1) maximum inelastic strain energy density and von Mises stress occur in the ball in the middle of the diagonal row; and 2) von Mises stress is almost equally distributed among all balls. However, when hyperbolic sine creep model is used, the obtained results are consistent with the observations in conventional solder ball WLP. Nevertheless, both creep models predict the significant reduction in solder ball stress and accumulated creep strain or inelastic strain energy density for hollow ball WLP. Existing experimental results of polymer-cored WLP from literature can indirectly validate the benefit from hollowed balls.

References

1. Fan, X.J., Varia, B., Han, Q., Design and optimization of thermo-mechanical reliability in wafer level packaging, Microelectronics Reliability, 50, 536–546, 2010.
2. Fan, X.J. and Liu, Y., Design, Reliability and Electromigration in Chip Scale Wafer Level Packaging, ECTC Professional Development Short Course Notes, 2009.
3. Fan, X.J. and Han, Q., Design and reliability in wafer level packaging, Proc of IEEE 10th Electronics Packaging Technology Conference (EPTC), 834-841, 2008.
4. Rahim, M.S.K., Zhou, T., Fan, X.J., Rupp, G., Board level temperature cycling study of large array wafer level packages, Proc of Electronic Components and Technology Conference (59th ECTC), 898-902, 2009.
5. Reche, J.H.J. and Kim, D.H., Wafer level packaging having bump-on-polymer structure, Microelectronics Reliability, 43, 879–894, 2003
6. Varia, B., Fan, X.J. and Han, Q., Effects of design, structure and material on thermal-mechanical reliability of large array wafer level packages, ICEPT-HDP, Beijing, 2009.
7. Kim D-H, Elenius P, Johnson M, Barrett S. Solder joint reliability of a polymer reinforced wafer level package, Microelectronics Reliability , 42,1837, 2002
8. Bumping Design Guide, [online], Available: http://www.flipchip.com/
9. Kawahara, T., SuperCSPs, IEEE Transactions on Advanced Packaging, v.23, No. 2, 2002
10. Gao, G., Haba, B., Organesian, V., Honer, H., Ovrutsky, D., Rosenstein, C., Axelrod, E., Hazanovich, F. and Aksenton, Y., Compliant WLP for enhanced reliability, International Wafer Level Package Conference, September 17-19 2007, San Jose, CA.
11. Eagelmaier, W., Achieving solder joint reliability in a lead-free world – part 2, Global SMT & Packaging, v.7, 2007, 45-46, [online], available: www.globalsmt.net/documents/Columns-Engelmaier/7.7_engelmaier.pdf
12. Okinaga, N.; Kuroda, H.; Nagai, Y., Excellent reliability of solder ball made of a compliant plasticcore, Electronic Components and Technology Conference, 1345 – 1349, 2001.
13. Keser, B.; Yeung, B.; White, J.; Fang, T., Encapsulated double-bump WL-CSP: design and reliability, ECTC 2001, 35-39.
14. Mitsuka, K.; Kurata, H.; Jun Furukawa; Takahashi, M., Wafer process chip scale package consisting of double-bump structure for small-pin-count packages, ECTC, 572 – 576, 2005.
15. Liu, X. and Lu, G.Q., Effects of solder joint shape and height on thermal fatigue lifetime, IEEE Trans. Comp. Packag. Technol., 26(2), 455-465, 2003.

16. Lim, S.S., Rajoo, R. and Wong, E.H., Reliability performance of stretch solder interconnections, in Proc. IEMT, 2006.
17. Anand, L., Constitutive equations for hot working of metals, J. Plasticity, 1, pp. 213–231, 1985.
18. Reinikainen, T.O, Marjamäki, P., Kivilahti, J.K., Deformation characteristics and microstructural evolution of SnAgCu solder joints, EuroSimE, 2005.
19. Lau, J., and W. Dauksher, Creep Constitutive Equations of Sn(3.5-3.9)wt%Ag(0.5-0.8)wt%Cu Lead-Free Solder Alloys, in Micromaterials and Nanomaterials, edited by B. Michel, IZM, Berlin, Germany, 2004, pp. 54-62.
20. Fan, X. J., Pei, M., and Bhatti, P.K., Effect of finite element modeling techniques on solder joint fatigue life prediction of flip-chip BGA packages, Proc. Of IEEE Electronic Components and Technology Conference (ECTC), 2006, May 30 - June 2, San Diego, CA, 2006
21. Darveaus, R., Solder Joint fatigue Life Model, Proceedings of the TMS Annual Meeting, pp.213-218, 1997
22. Syed, A., Predicting Solder Joint Reliability for Thermal, Power, & Bend Cycle within 25% Accuracy, 51st ECTC, pp. 255-263, 2001
23. Pei, M., Fan, X.J., Bhatti, P.K., Field condition reliability assessment for SnPb and SnAgCu solder joints in power cycling including mini cycles, Proc. of Electronic Components and Technology Conference (ECTC), 899-905, 2006
24. Bhatti, P.K., Pei, M., Fan, X.J., Reliability analysis of SnPb and SnAgCu solder joints in FC-BGA packages with thermal enabling preload, Proc. of Electronic Components and Technology Conference (ECTC), 601-606. 2006.
25. Fan, X.J., Rasier, G., Vasudevan, V.S., Effects of dwell time and ramp rate on lead-free solder joints in FCBGA packages, Proc. of Electronic Components and Technology Conference (ECTC), 901-906, 2005.
26. Vasudevan, V., Fan, X., Liu, T., Young, D., Slow cycle fatigue creep performance of Pb-Free (LF) solders, Proc of Electronic Components and Technology Conference (ECTC), 116-123, 2007.